Available online at www.sciencedirect.com
ScienceDirect
Dyes and Pigments 75 (2007) 408–412
DYES and PIGMENTS
www.elsevier.com/locate/dyepig

Fluorescence and electrochemical properties of naphthylporphyrins and porphyrin–anthraquinone dyads

Minli Tao [a], Xueqin Zhou [a], Ma Jing [a], Dongzhi Liu [a,*], Jun Xing [b]

[a] School of Chemical Engineering and Technology, Tianjin University, Tianjin 300072, China
[b] Library Center, Tianjin Medical university, Tianjin 300070, China

Received 20 February 2006; received in revised form 13 March 2006; accepted 8 June 2006
Available online 27 November 2006

Abstract

Porphyrins bearing naphthyl group were synthesized to afford expanded π-conjugated systems and were characterized by ^{1}H NMR, IR, FAB-MS and UV–vis spectra. The fluorescence spectra illustrate that the maximal excitation and emission wavelengths of naphthylporphyrins were red shifted with 3–6 nm compared with that of **H_2TPP**. The cyclic voltammetric results of 8 kinds of naphthylporphyrin are firstly reported. Several porphyrin–anthraquinone dyads were synthesized and their molecular energy levels were obtained from the multilevel ionization potential (IP) and electron affinity (EA) according to the redox potential. Photoinduced intramolecular electron transfer occurred from porphyrin ring to anthraquinone moiety, which was confirmed by fluorescence quenching and molecular energy level changing.

Keywords: Porphyrin; Anthraquinone; Ionization potential; Electron affinity; Cyclic voltammograms; Fluorescence quenching

1. Introduction

Porphyrin derivatives, that can be preferentially taken up by the tumor tissue and effectively accumulated within tumor cells for a long period of time [1–7], have attracted the biological researchers. Moreover, porphyrins produce highly reactive oxygen species (e.g. $^1O_2$) when excited by an appropriate wavelength light, hence it could destroy the tumor cells [8]. Presently, porphyrin derivatives have been used as photosensitizers for photodynamic therapy of cancer, cardiovascular and ophthalmic diseases [9–11]. However, in order to obtain better therapy, chemical drugs should be used combined with photosensitizers for clinical purpose. One of these chemical drugs is anthraquinone derivative, which is photoactive too, and which could be inserted between the two base pairs of DNA helix and could cause a local untwisting of the helix, resulting in miscoding and possible cell death to accomplish the chemical therapy for cancer [12]. To simplify the therapy process, it is considered to combine both into one dyad. In other words, introduction of anthraquinone unit to porphyrin molecules is expected to be a novel anticancer target-drug. Firstly utilization of a photoactive, intercalatable moiety in conjunction with porphyrin chromophore might accentuate the photochemical activity of the dyad molecules leading to an efficient DNA cleavage as reported [13,14] by Mehta et al. Moreover, electron transfer between porphyrin and anthraquinone [15,16] would be induced when exposed to light, leading to the breaking up of the dyads. That is to say the dyads could decompose to their original compounds to achieve their own therapy – the ''photodynamic therapy'' of porphyrin and the ''chemical therapy'' of anthraquinone, respectively.

The common porphyrin photosensitizers also distribute in non-focus. Since the accumulation of photosensitizers in body may last up to 4–6 weeks, the undesirable post-treatment phototoxic response would be a problem clinically. To lower the photo-toxicity, the porphyrins are required to improve its focus–target properties. It is reported that highly aromatic groups, such as naphthyl, substituted in the *meso* positions

* Corresponding author. Tel./fax: +86 22 27400911.
E-mail address: dzliu@tju.edu.cn (D. Liu).

0143-7208/$ - see front matter © 2006 Elsevier Ltd. All rights reserved.
doi:10.1016/j.dyepig.2006.06.022

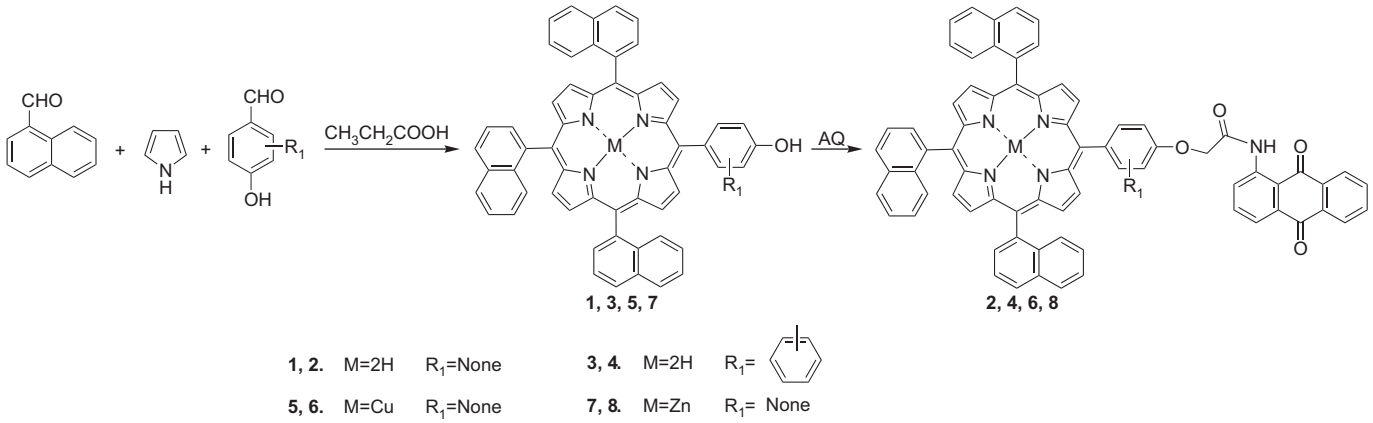

Scheme 1. Synthesis of naphthylporphyrins and porphyrin–anthraquinone dyads.

may endow porphyrins with increased tumor localization properties [17]. Therefore, this paper focused on the investigation of porphyrins bearing naphthyl group and their anthraquinone derives. The porphyrin derivatives were synthesized as depicted in Scheme 1. The fluorescence properties and electrochemical properties were investigated in detail.

2. Experiment

2.1. General

4-Hydroxy-1-naphthaldehyde, chloroacetyl-α-aminoanthraquinone (**AQ**), *meso*-tetraphenylporphyrin (**H_2TPP**) and *meso*-tetra-α-naphthylporphyrin (**H_2TNP**) were prepared as reported [18–20]. Compounds **1**, **2**, **3**, **5** and **6** were prepared in the laboratory and their synthesis were reported in literature [21]. All other reagents and solvents were reagent grade and further purified by the standard methods if necessary. Infrared spectra were recorded on a Bio-Rad FTS3000. ^{1}H NMR spectra were obtained on a Varian UnityPlus400 spectrometer. Mass spectra were depicted on a VG ZAB-HS mass spectrometer. Absorption spectra were taken on a Thermo Spectronic, Helios Gamma UV–Visible spectrophotometer. Fluorescence spectra were recorded on a Varian Cary Eclipse fluorospectrophotometer. Solid fluorescence was observed by Olympus BH-2 fluorescence microscope. Electrochemical properties were measured using BAS 100 W electrochemical analyzer and were performed in a three-electrode cell in this paper. Glassy carbon electrode was used as working electrode, saturated calomel electrode (SCE) as reference electrode and platinum as auxiliary electrode. Scan rates were 50–200 mV/s. Dichloromethane with 0.05 M tetra-butylammonium perchlorate was employed as the medium for all the cyclic voltammetric experiments.

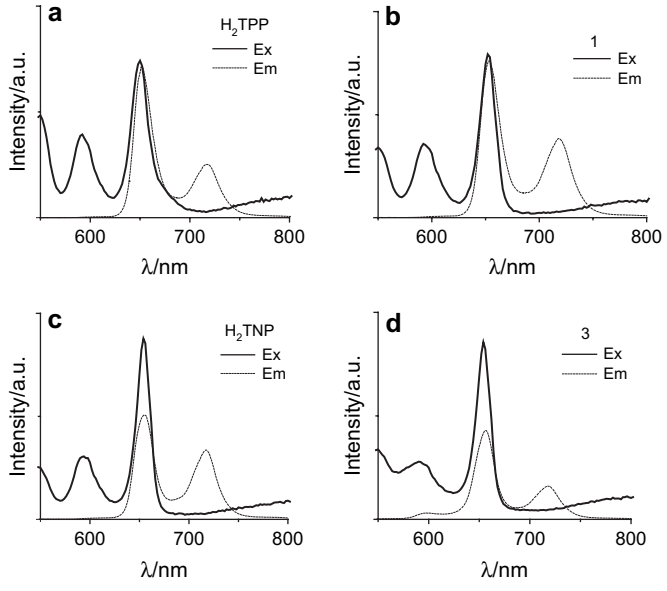

Fig. 1. Mirror-image symmetry between absorption and emission spectra. (a) '—' (solid line) is the absorption spectra of **H_2TPP**, '⋯' (dotted line) is the emission spectra of **H_2TPP**; (b) '—' is the absorption spectra of compound **1**, '⋯' is the emission spectra of compound **1**; (c) '—' is the absorption spectra of **H_2TNP**, '⋯' is the emission spectra of **H_2TNP**; (d) '—' is the absorption spectra of compound **3**, '⋯' is the emission spectra of compound **3**.

2.2. Synthesis of 5-[4-(α-imineanthraquinone-acetyl)-methoxynaphthyl]-10,15,20-tri(α-naphthyl) porphyrin (*4*)

In a 100 mL round bottom flask with reflux condenser, a mixture of compound **3** (174 mg, 0.21 mmol) and K_2CO_3 (0.4 g) in dry DMF (30 mL) was heated to 85 °C for 10 min.

Table 1
Fluorescence data of naphthylporphyrins in CH_2Cl_2 (5×10^{-6} mol/L)

Compound	E_x (nm)	E_m (nm)		$I_{\lambda1}/I_{\lambda2}$	Q%	E_g (eV)
H_2TPP	423	651	717	2.83	–	1.91
H_2TNP	428	655	717	1.51	–	1.89
1	426	653	718	1.98	–	1.90
2	428	651	718	1.57	22	1.91
3	428	657	718	2.67	–	1.89
4	426	650	717	1.74	32	1.91
7	424	596	646	0.48	–	1.93
8	426	595	645	0.39	24	1.94

E_x is the maximal excited wavelength; E_m is the maximal emission wavelength; $I_{\lambda1}$ is fluorescence intensity at the first emission wavelength; $I_{\lambda2}$ is fluorescence intensity at the second emission wavelength; Q% is fluorescence-quenching percent; E_g is the band gap obtained from edge absorption.

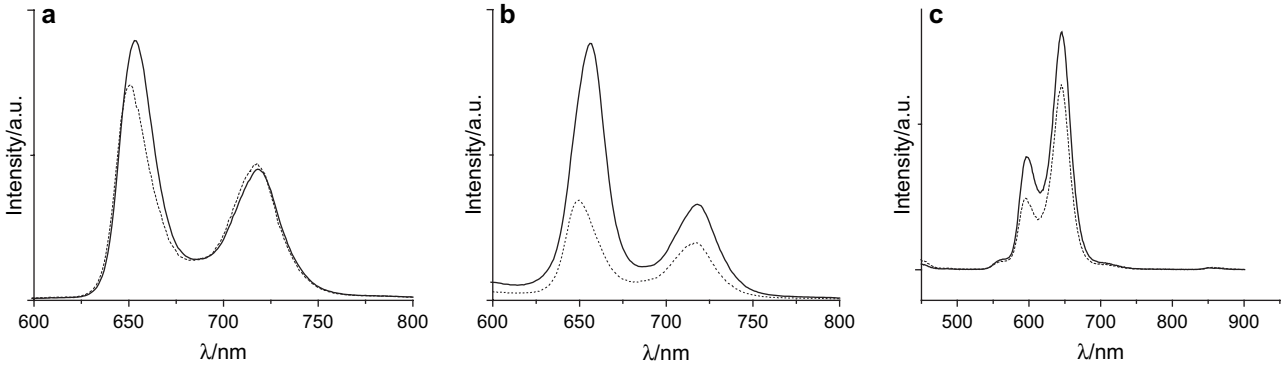

Fig. 2. Fluorescence emission spectra of the naphthylporphyrin and porphyrin–anthraquinone dyads. (a) '—' (solid line) is the emission spectra of compound **1**, '⋯' (dotted line) is the emission spectra of the dyad **2**; (b) '—' is the emission spectra of compound **3**, '⋯' is the emission spectra of the dyad **4**; (c) '—' is the emission spectra of compound **7**, '⋯' is the emission spectra of the dyad **8**.

Then **AQ** (80 mg, 0.25 mmol) was added and the mixture was stirred at 85–90 °C for 5 h. After the reaction gets completed, the reaction mixture was evaporated in vacuum. Compound **4** was isolated in 51% yield by column chromatography of the residue on silica gel eluting with chloroform–ethanol (150:1 v/v).

IR (KBr): 3318 (γ_{N-H}), 1337 ($\gamma_{C=N}$), 1273 (γ_{C-O-C}), 1647, 1673, 1701 ($\gamma_{C=O}$), 1508, 1578 ($\gamma_{C=C}$), 793, 734 cm^{-1}; ^1H NMR ($CDCl_3$) δ: 13.61 (s, 1H), 9.41 (d, 1H), 8.60–8.48 (m, 8H), 8.35–8.19 (m, 11H), 7.97–7.92 (m, 5H), 7.82–7.74 (m, 5H), 7.61–7.55 (m, 6H), 7.45–7.27 (m, 6H), 5.25 (s, 2H), −2.38 (s, 2H); MS (FAB) *m/z*: 1094.4(M^+); λ_{max}: 425 nm (ε 205, 200), 517 (11,800), 551 (4600), 594 (4000) 649 (2000).

*2.3. Synthesis of zinc(II) 5-(4-hydroxy-phenyl)-10,15,20-tri(α-naphthyl) porphyrin (**7**)*

A chloroform solution (5 mL) of compound **1** (40 mg, 0.05 mmol) was added to a chloroform and methanol solution of zinc acetate (80 mg, 0.36 mmol). The mixture was stirred at refluxing temperature for 4–5 h with TLC monitoring the completion of the reaction. The solvent was removed and the residue was purified by column chromatography on silica gel eluting with CH_2Cl_2 to get dark red solid in 94% yield.

IR (KBr): 3510 (γ_{OH}), 1338 ($\gamma_{C=N}$), 1263 (γ_{C-O}), 1001 (porphyrin ring), 1506, 1591 ($\gamma_{C=C}$), 796, 719 cm^{-1}; ^1H NMR ($CDCl_3$) δ: 8.39 (s, 2H), 8.25 (s, 2H), 8.15 (s, 4H), 7.98–6.93 (m, 27H), 5.02 (s, 1H); MS (FAB) *m/z*: 894.4 (M^+); λ_{max}: 425 nm (ε 381,000), 550 (6200).

*2.4. Synthesis of zinc(II) 5-[4-(α-imineanthraquinone-acetyl)-methoxyphenyl]-10,15,20-tri(α-naphthyl) porphyrin (**8**)*

Compound **8** was prepared from compound **2** and zinc acetate in the same procedure as for the preparation of compound **7** and in 92% yield. IR (KBr): 1336 ($\gamma_{C=N}$), 1282 (γ_{C-O-C}), 1644, 1673, 1732 ($\gamma_{C=O}$), 1000 (porphyrin ring), 1505, 1577 ($\gamma_{C=C}$), 795, 708 cm^{-1}; ^1H NMR ($CDCl_3$) δ: 13.41 (s, 1H), 9.26 (s, 1H), 8.58–8.38 (m, 8H), 8.32–7.26 (m, 33H), 4.88 (2H, $-OCH_2$); MS (FAB) *m/z*: 1158.5 ($M^+ + 1$); λ_{max}: 425 nm (ε 327,600), 551 (17,800).

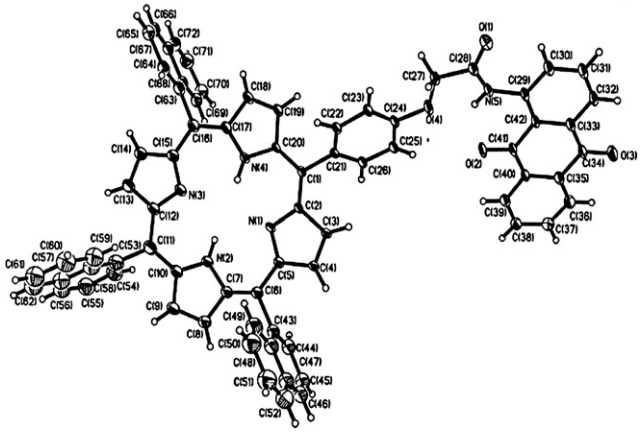

Fig. 3. X-ray structure of compound **2** (coordinated solvent are omitted for clarity).

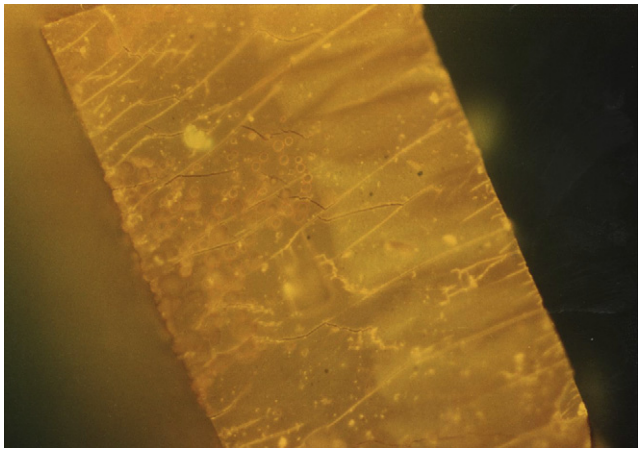

Fig. 4. Crystal solid fluorescence of compound **2** obtained from fluorescence microscope, taken by Olympus C-35AD-4 digital camera, excited by blue light and magnified for 40 times.

Table 2
Oxidation–reduction potential data of compounds

Compound	E_2^{red}	EA_2	E_1^{red}	EA_1	E_{AQ}^{red}	EA_{AQ}	E_1^{ox}	IP_1	E_2^{ox}	IP_2
H_2TPP	−1.77	−2.62	−1.46	−2.93			0.81	−5.20	1.13	−5.52
H_2TNP	−1.82	−2.57	−1.47	−2.92			0.79	−5.18	1.15	−5.54
1	−1.94	−2.45	−1.50	−2.89			0.76	−5.15	1.18	−5.57
2	−1.84	−2.55	−1.50	−2.89	−1.04	−3.35	0.78	−5.17	1.07	−5.46
3	−1.88	−2.51	−1.54	−2.85			0.77	−5.16	1.25	−5.64
4	−1.87	−2.52	−1.52	−2.87	−1.07	−3.32	0.74	−5.13	1.01	−5.40
5	–	–	−1.64	−2.75			0.75	−5.14	1.06	−5.45
6	–	–	−1.66	−2.73	−1.04	−3.35	0.77	−5.16	1.04	−5.43
7	–	–	−1.67	−2.72			0.60	−4.99	0.87	−5.26
8	–	–	−1.69	−2.70	−1.00	−3.39	0.57	−4.96	0.85	−5.24

E_1^{ox}, E_2^{ox} are the oxidation potentials; E_1^{red}, E_2^{red}, E_{AQ}^{red} are the reduction potentials; IP_1, IP_2 are the ionization potentials; EA_1, EA_2, EA_{AQ} are the electron affinities.

3. Results and discussion

3.1. Fluorescence

3.1.1. Fluorescence spectra

The emission spectra of compounds **1** and **2** are similar to that of **H_2TPP** and **H_2TNP**, which have reverse mirror-image symmetry between absorption and emission spectra, and they are shown in Fig. 1.

After the combination of Cu^{2+} with porphyrin ring, the Cu-complexes keep a single electron state at the outer layer, which could explain the fluorescence vanishing. The fluorescence data of other compounds are given in Table 1 and Fig. 2. The maximal excitation wavelength of naphthylporphyrins was red shifted with 3–5 nm compared with that of **H_2TPP**. Furthermore, the red shift was also observed in the emission wavelength because of the expansion of the π-conjugated system in naphthylporphyrins. These results also indicate that the energy gap between the ground state and the excited state of naphthylporphyrins was decreased and they should be excited more easily.

The fluorescence quenching percent (Q%) could be calculated on the basis of the relative fluorescence intensity and rectified by the absorption of the excitation wavelength. The fluorescence quenching occurred in compounds **2**, **4**, and **8** compared with the corresponding original compounds **1**, **3**, and **7** are, respectively, up to 22%, 32% and 24%. The fluorescence emission spectra are shown in Fig. 2. However, no quenching was found in the mixture **AQ** and the corresponding original porphyrins. This implies that photoinduced intramolecular electron transfer occurs from the excited porphyrin singlet state to the appended anthraquinone, resulting in the fluorescence quenching in compounds **2**, **4** and **8**.

3.1.2. Solid fluorescence

The accumulated blue piece single crystal of compound **2** was obtained from chloroform–heptane (6:1 v/v) under heptane vapour. The X-ray crystal structure of which is shown in Fig. 3. When we observe the single crystal using fluorescence microscope, it displays a beautiful solid fluorescence. The crystal lighted by blue ray for 10 min and magnified for 40 times is shown in Fig. 4.

3.2. Electrochemical properties

The redox potential of the compounds are summarized in Table 2 and the cyclic voltammograms for some compounds are shown in Fig. 5. For comparison, *meso*-tetraphenylporphyrin (**H_2TPP**) and *meso*-tetra-α-naphthylporphyrin (**H_2TNP**) were also examined under the same conditions.

Naphthylporphyrins **H_2TNP**, **1** and **3** all exhibit four pair redox peaks and they are ascribed to the first and second redox process of porphyrin ring. The first oxidation peaks of naphthylporphyrins (E_1^{ox} = 0.79, 0.76, 0.77) shift to a lower potential compared to the phenylporphyrin **H_2TPP** (E_1^{ox} = 0.81). This result illustrate that the naphthylporphyrins are easier to be oxidized than phenylporphyrin. The introduction of naphthyl group and the enhancement of the conjugation degree of the porphyrins could account for these potential shifts phenomena. The expansion of the π-conjugated system causes HOMO to shift to higher energy and consequently cause the potential shift.

From Fig. 5 we can find that the cyclic voltammogram of the compounds **2** exhibited a favorable reversible process. Reversible oxidation peaks were observed at E_1^{ox} = 0.78 V and E_2^{ox} = 1.07 V assigned to the first and second oxidation of porphyrin unit. On the reduction side, there are three reversible peaks: E^{red} = −1.04, −1.50, −1.84 V, corresponding to the reduction of anthraquinone group and the first and second reduction of porphyrin ring. The reduction peak of E_{AQ}^{red} = −1.07 of compound **4** indicates the appearance of new redox process in the system as well as in compound **2**.

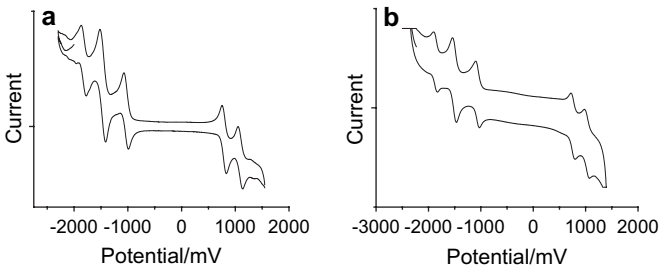

Fig. 5. Cyclic voltammograms of compounds. (a) Cyclic voltammogram of compound **2**; (b) cyclic voltammogram of compound **4**.

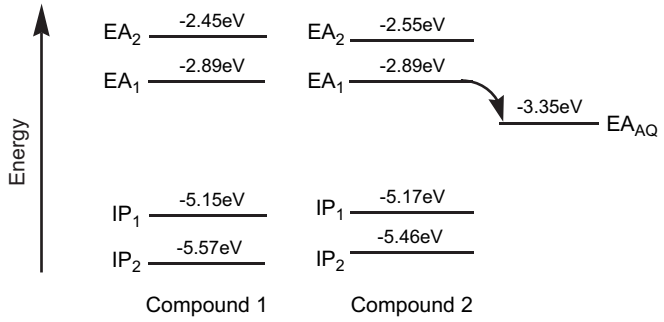

Scheme 2. Schematic energy diagram of porphyrin **1** and porphyrin–anthraquinone dyad **2**.

For the metal porphyrin, there are two oxidation peaks and one reduction peak belonging to the porphyrin ring. Their anthraquinone derivatives **6** and **8** exhibit anthraquinone reduction peaks at $E^{red}_{\mathbf{AQ}} = -1.04,\ -1.00$. The oxidation potential value of compounds **7** ($E^{ox}_1 = 0.60,\ E^{ox}_2 = 0.87$) and **8** ($E^{ox}_1 = 0.57,\ E^{ox}_2 = 0.85$) are lower than the corresponding compounds **1** and **2**, which could be explained by the introduction of metal Zn.

The first ionization potential (IP_1) is defined as the removal of an electron from the ground state of a molecule and this process corresponds to the first oxidation process. Removing of another electron from the univalent cation is called the second ionization potential (IP_2). Similarly, the IP_2 corresponds to the second oxidation potential. On the contrary, the first electron affinity (EA_1) is the process of obtaining an electron by the ground state of a molecule and associated with the first reduction process. Moreover, the second electron affinity (EA_2) is associated with the second reduction process. Herein, the multilevel ionization potential (IP_n) and the multilevel electron affinity (EA_n) of porphyrin ring were calculated based on the corresponding oxidation and reduction potentials as follows according to literature [22]: $IP_n = -eE^{ox}_n - 4.39$ eV; $EA_n = -eE^{red}_n - 4.39$ eV. Because the anthraquinone group was bonded by single bond with porphyrin, the electron affinity of which was calculated separately and recorded as $EA_{\mathbf{AQ}}$. The experimental data are summarized in Table 2. According to the results, schematic energy diagram could be drawn as in Scheme 2 to illustrate the changing of energy due to the introduction of anthraquinone groups (with compounds **1** and **2** as example).

$EA_{\mathbf{AQ}}$ is the additional energy level because of the introduction of anthraquinone group. In common porphyrin compound, the excited electron in energy level EA_1 would combine with charges in IP_1 to emit the fluorescence, such as compound **1**. While in the dyad **2**, the excited electron can also hop to the energy level $EA_{\mathbf{AQ}}$. This result indicates that the photoinduced intramolecular electron transfer might occur from the excited porphyrin ring to the appended anthraquinone moiety, which is consistent with the fluorescence quenching experiment.

4. Conclusion

In summary, the fluorescence measurement suggested that the introduction of naphthyl group could enhance the π-conjugated system of porphyrins and the electrochemical results confirm this point by exhibiting the more negative oxidation potentials. Furthermore, the photoinduced intramolecular electron transfer in the porphyrin–anthraquinone dyads could accelerate the breaking up of chemical bond and make the decomposition of the dyads possible. So these porphyrin–anthraquinone dyads may be used as novel anticancer drug with double efficacy of ‘‘photodynamic therapy’’ and ‘‘chemical therapy’’.

References

[1] Ali H, van Lier JE. Chem Rev 1999;99:2379.
[2] Bonnett R, Martínez G. Tetrahedron 2001;57:9513.
[3] Kim YS, Song R, Kimb DH. Bioorg Med Chem 2003;11:1753.
[4] Boyle RW, Dolphin D. Photochem Photobiol 1996;64:469.
[5] James DA, Swamy N, Paz N, Hanson RN, Ray R. Bioorg Med Chem Lett 1999;9:2379.
[6] Bonnet R. Chem Soc Rev 1995;19.
[7] Dolphin D. Can J Chem 1994;72:1005.
[8] Pandey SK, Gryshuk AL, Graham A, Ohkubo K, Fukuzumi S, Dobhal MP, et al. Tetrahedron 2003;59:10059.
[9] Sternberg ED, Dolphin D. Tetrahedron 1998;54:4151.
[10] Milanesio ME, Morán FS, Yslas IE. Bioorg Med Chem 2001;9:1943.
[11] Nishiyama N, Stapert HR, Zhang GD. Bioconjugate Chem 2003; 14:58.
[12] Johnson MG, Kiyokawa H, Tani S, Koyama J, Morris-Natschke SL, Lee KH. Bioorg Med Chem 1997;5:1469.
[13] Mehta G, Muthusamy S, Maiya BG. Tetrahedron Lett 1997;38:7125.
[14] Breslin DT, Coury JE, Anderson JR. J Am Chem Soc 1997;119:5043.
[15] Wiehe A, Senge MO. Tetrahedron 2001;57:10089.
[16] Senge MO, Rößler B, Jörg VG. Tetrahedron Lett 2004;45:3363.
[17] Kaelin AC, Zanelli GD. J Label Compd Radiopharm 1989;28:343.
[18] Lindsey JS, Hsu HC, Schreiman IC. Tetrahedron Lett 1986;27:4969.
[19] Bhargava PN, Raghvan Nair MG. J Indian Chem Soc 1957;34:42.
[20] Adler AD. J Org Chem 1967;32:476.
[21] Tao ML, Liu DZ, Zhou XQ. Chin J Appl Chem 2004;21:479.
[22] Li YF, Cao Y, Gao J. Synth Met 1999;99:243.